Modelling Ethnogenesis

Alexey Piunovskiy[1] and Bakhtier Vasiev[2]

Department of Mathematical Sciences, University of Liverpool, L69 7ZL, UK.
[1]piunov@liverpool.ac.uk, [2]bnvasiev@liverpool.ac.uk

Abstract

One of the fundamental problems of contemporary history is to understand the processes governing the rise and fall of polities. The universality of boom-and-bust dynamics associated with the life-cycle of polities tempts to treat the problem mathematically and thus brings it to the framework of cliodynamics. Here we introduce a mathematical model of evolving polity under assumption that its evolution is associated with interactions of certain groups of people, forming the polity and differing by their psycho-ethic characteristics. The model is given in terms of ordinary differential equations and the bust dynamics associated with the rise and fall of polities is modelled as an excitation process, which is the non-linear phenomenon, well known in mathematical biology. We consider the deterministic as well as the stochastic version of the model which we fit to the time-scale of civilization's lifespan. We also expand the model to study interaction between two evolving polities. Investigation is performed using analytical methods as well as numerical integration (i.e. MATLAB simulation).

Keywords: Ethnogenesis, Population Dynamics, Dynamical System, Excitation
AMS 2020 subject classification: 37N25, 37M05, 92B05, 92D15, 92D25

1 Introduction

From ancient times till 19th century historical processes have been considered as resulting from actions of extraordinary people. The concept of natural laws underlying historical processes (in terms of historical necessity as opposing to free will of heroes) was expressed by Leo Tolstoy in the forth volume of "War and Peace" [20] and, to a certain extent, by Lion Feuchtwanger in his historical novel "Raquel, the Jewess of Toledo" [5]. Cyclicity of historical processes indicated by the rise and fall of civilizations was brought to consideration of scientists in early twentieth century by Oswald Spengler [17]. Following his work, all history of mankind in the last 5 thousand years can be viewed in terms of rises and falls of civilizations.

One of the challenges of contemporary science is to uncover social laws (or mechanisms) governing the dynamics of evolving polities, including multi-ethnic polities or civilizations. Arnold Toynbee in his book "A study of History" [21] has analysed the formation of 26 civilization and concluded that their success was ensured by leadership of a small group of elites. The idea that the collective action of a group of people (sized between one individual and an entire polity) drives the evolution of polity, was explored to a great extent by many researchers. Such collective action has been viewed as grounded on collective solidarity [7], social cohesion (or collectivism) [22], social capital (or social trust) [16] and other social or psycho-ethic characteristics of subgroups forming polities.

Remarkably, the concept of collective solidarity was introduced by Arabic historian Ibn Khaldun in the 15th century [11]. In his research he got far ahead of his time: on the basis of known history of Maghreb, Arabic Spain and Middle East he concluded that the growth and evolution of a polity is based on collective action of a certain subgroup of people having higher level of collective solidarity, which he called "asabiya". Ibn Khaldun stated that the level of asabiya is higher among people inhabiting the geographic periphery of the polity rather than the inner land. The concept of asabiya together with the above statement were used by Peter Turchin for the development of

mathematical model (the so-called Metaethnic Frontier Theory [23]) which allowed to reproduce and explain the boom-and-bust dynamics of evolving polity. It is worth noting here that the models based exclusively on geopolitical statements [1, 3] did not allow the reproduction of such dynamics.

One of contemporary metahistoric theories was suggested by Lev Gumilev [8, 9]. He considered each civilization as a manifestation of particular ethnos, which, under certain conditions, appears and builds civilization, but with time gets old and dies, causing the associated civilization to disappear. According to Gumilev's theory [8, 9] the driving force for formation of a new ethnos comes from a certain group of people, whom he calls "passionaries" or people with drive. This group is considered as a fraction of population habitating certain geographic territory, who express high levels of passion and lead their fellows (i.e. tribesmen), forming the rest of the population to expand and to build a new society (civilization).

According to Gumilev [8, 9] the formation and death of a civilization can be described by the dynamics of civilization's "passionary tension" or drive, which he illustrated by a "bust" curve shown in Figure 1. It starts with a growing phase (rise of civilization) followed by plateau (ackmatic phase), fast decline (breaking phase), slow decline (inertial obscuration) and low level tail (obscuration or regeneration-relict). The entire process, which according to Gumilev takes about 15 centuries, can be considered as a response to a disturbance, caused by initiation of a small fraction of passionaries. Such response is known in physiology as excitation [13, pp.239-242], that is when a small perturbation to the system results in a full-sized response.
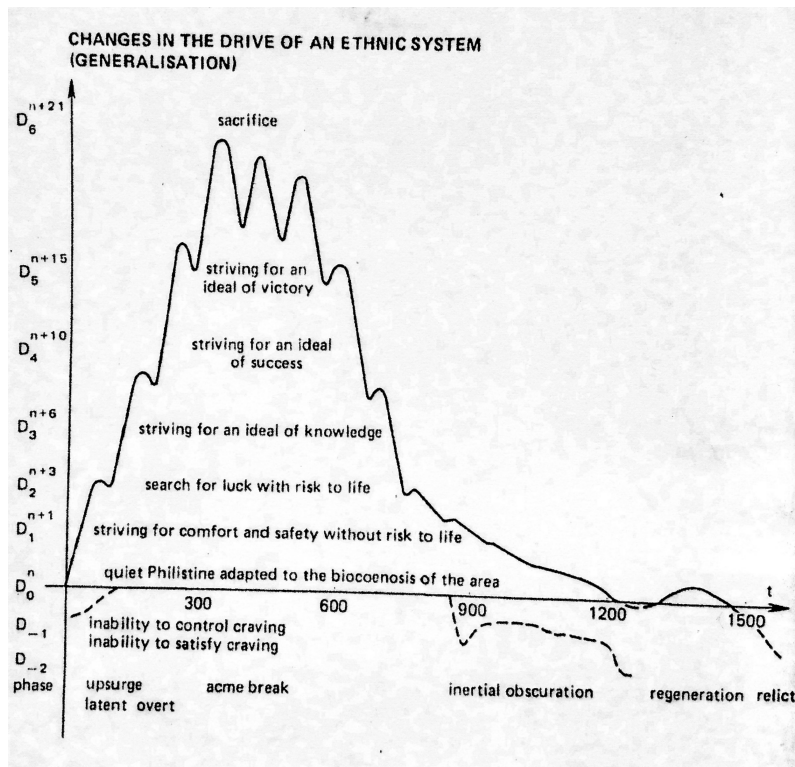

Figure 1: Graphical illustration of the evolution of an ethnos (civilization) [8, p.240].

The aim of the current article is to develop a mathematical model which would explain the boom-and-bust dynamics (which is evident from Figure 1) exhibited in the course of ethnogenesis. We note that Gumilev's theory led to the mathematical model presented in [10]. The main variable describing the dynamics of the polity in this model was the so-called "passionary tension" similar to the variable quantifying asabiya in Methaethnic Frontier Theory [23]. The main drawback of the model presented in [10] is that it is given by a system of seven nonlinear differential equations containing more than thirty variables. Although the authors were able to find a set of model parameters that allowed them to reproduce the boom-and-dust dynamics, no further explanations

and investigations of this dynamics were made. Contrary to the previous studies we put an association of the boom-and-bust dynamics with the type of system's nonlinearity known as excitability. The excitable dynamics in the model describing the ethnogenesis is the main theme of the current work. We will build a mathematical model of ethnogenesis, which is based on the statements from Gumilev's theory.

- According to Gumilev there are three main subgroups in the population that have different behavioural patterns and affect the evolution of the ethnos. The driving force for the growth of populations and further improvements resulting in the rise of a civilization comes from passionaries, whose idealistic motivations are grounded in altruism. The bulk of population is represented by harmonious individuals who work on preservation of the current state of the ethnos. There is also a destructive group of individuals, called subpassionaries (or people with negative drive – vargants, mercenaries, degenerates), who are as active as passionaries but whose actions are based on egoism rather than altruism.

- The formation of a new ethnos (or civilization) is associated with initiation of passionaries. Gumilev describes conditions under which passionaries appear and take over the population, but we will not go into details of these conditions and will postulate that at a certain time, a small fraction of population is already represented by passionaries.

We will design a few models describing the ethnogenesis. In the first model we will consider the population as consisting of two subgroups, namely, the passionaries and the remainder of the population. This two-variable model will let us identify possible interactions between these subgroups which allow the bust dynamics in the course of ethnogenesis. In the second version of the model we will consider all three subgroups and analyse the interactions between them which is consistent with the observed dynamics during ethnogenesis. In the follow up steps of our research we will use the three-variable model for the study of the impact of noisy environment on the ethnogenesis. Particularly we show that the noise is amplified by nonlinearities in the model. Finally, we extend the three variable model (with noise) to consider interaction between two ethnogenetic processes taking place simultaneously, with a certain time lag. This allows us to model conflicting civilizations and to identify conditions when one of them takes over the other.

2 Two-Variable Model

As a starting point we will consider the two-variable model:

$$\begin{cases} \dot{x} = xf(x,y) \\ \dot{y} = yg(x,y) \end{cases} \tag{1}$$

where variable x represents the size of the subpopulation formed by passionaries while y is the size of the remaining population (which includes both harmonious people and subpassionaries). Equation (1) is commonly used for modelling population dynamics in biology, where x and y are considered as the sizes of two biological species. Using linear approximation of functions $f(x,y)$ and $g(x,y)$ we get:

$$\begin{cases} \dot{x} = x(a_0 + a_1 x + c_1 y); \\ \dot{y} = y(b_0 + b_1 y + d_1 x), \end{cases} \tag{2}$$

which is a generalised representation of the Lotka-Volterra model [25, 26]. Commonly this model is considered under the following condition for model parameters: $a_0 > 0$, $b_0 > 0$ while $a_1 < 0$ and $b_1 < 0$ preventing unlimited growth of populations. After nondimensionalisation this equation is commonly transferred into

$$\begin{cases} \dot{x} = x(1 - x + \beta_1 y); \\ \dot{y} = \gamma y(1 - y + \beta_2 x), \end{cases} \tag{3}$$

where γ defines the relative rate of change of y with respect to x [13, p.119]. If $\beta_{1,2} = 0$ the two equations are detached and both species exhibit logistic growth. Furthermore, depending on the signs of these two parameters the model reproduces three types of interactions between populations

3

x and y, namely, predator-pray ($\beta_1 > 0$, $\beta_2 < 0$), symbioses ($\beta_1 > 0$, $\beta_2 > 0$) and competition ($\beta_1 < 0$, $\beta_2 < 0$) [25]. The model allows four equilibria and in case of competitive Lotka-Volterra model ($\beta_1 < 0$, $\beta_2 < 0$) all four equilibria are meaningful and correspond to non-negative sizes of populations. These are the trivial equilibrium ($x = 0$, $y = 0$), the extinction of y-population ($x \neq 0$, $y = 0$), the extinction of x-population ($x = 0$, $y \neq 0$) and the co-existence ($x \neq 0$, $y \neq 0$). Depending on model parameters, the solution of the system converges either to the co-existence of species or to the case when one of them becomes extinct [13, pp.104-126].

In our case we would like for one of the variables, say x, to represent the size of the subpopulation formed by passionaries, while y is the size of the remaining part of population (which would include harmonious people and subpassionaries). We expect to observe the excitation dynamics. Since the excitation in biology is known to be a non-linear process, we will need more than just a linear expansion of functions $f(x, y)$ and $g(x, y)$ in (1). The simplest way is to add one quadratic term into the first equation which transforms our system to

$$\begin{cases} \dot{x} = x(a_0 + a_1 x + a_2 x^2 + c_1 y); \\ \dot{y} = y(b_0 + b_1 y + d_1 x). \end{cases} \tag{4}$$

There are up to six equilibria in this system of which two are always real:

$$(x_1, y_1) = (0, 0), (x_2, y_2) = (0, -b_0/b_1).$$

These two equilibria are located on the vertical axis. Two more equilibria (if real) are located on the horizontal axis:

$$(x_{3,4}, y_{3,4}) = \left(\frac{-a_1 \pm \sqrt{a_1^2 - 4a_0 a_2}}{2a_2}, 0 \right). \tag{5}$$

And, finally, two remaining equilibria (if real) are represented by the points of intersection of the line $b_0 + b_1 y + d_1 x = 0$ with parabola $a_0 + a_1 x + a_2 x^2 + c_1 y = 0$. To set an excitable kinetics in the system (4) we make sure that the equilibrium (x_2, y_2) is stable and located in the vicinity of the parabola $a_0 + a_1 x + a_2 x^2 + c_1 y = 0$. The excitable dynamics becomes more evident after nondimensionalisation of the system (4) (so that $a_2 = -1$) and transferring it into the following form:

$$\begin{cases} \dot{x} = x((1-x)(x-\alpha) + \beta_1(y - y_0)); \\ \dot{y} = \gamma y(y_0 - y + \beta_2 x), \end{cases} \tag{6}$$

where parameters γ, β_1 and β_2 have the same meaning as those in the equation (3), new parameter α defines the excitation threshold of the system and y_0 defines the location of the equilibrium $(x_2, y_2) = (0, y_0)$ which is stable if β_1 and β_2 have opposite signs. Note, that the parameters α, y_0 and γ should all be positive. It looks that, in any case, the system (6) with positive initial conditions admits a unique bounded solution on the infinite horizon $[0, \infty)$. For $\beta_1 \leq 0$, $\beta_2 \geq 0$, this will follow from the investigation of the three-variable model (7). Concerning the equilibria in the system (6), we note that the trivial steady state $(x_1, y_1) = (0, 0)$ is unstable (saddle). Furthermore, if the parabola $(1-x)(x-\alpha) + \beta_1(y - y_0)$ has real and non-negative roots, then the system (6) has two meaningful equilibria located on the horizontal axis (same as given by (5)) and for the concave up parabola the equilibrium which is closer to the origin (smaller x-coordinate) is the unstable node, while the other one is a saddle. For simplicity, we consider the cases when the nullcline represented by the parabola $(1-x)(x-\alpha) + \beta_1(y - y_0) = 0$ doesn't intersect the one given by the line $y_0 - y + \beta_2 x = 0$ and therefore we don't have any extra equilibria.

The dynamics in the system (6) is illustrated by Figure 2. Null-clines of the system are shown in blue on panel A. These null-clines indicate the excitable nature of the system (6) and this is illustrated by a set of phase trajectories (shown in red) coursed by the perturbation of the system from its stable equilibrium $(x_2, y_2) = (0, y_0)$. Any perturbation from this state results in the relaxation of the system back to this equilibrium. However if the perturbation is above certain threshold, for example, if the initial value of y is equal to y_0 and the initial value of x is above α, then the perturbation increases further before the system relaxes back to the stable equilibrium (x_2, y_2).

The dynamics of variables x and y over time for one of the phase trajectories (starting from the point $x_0 = 0.1$ and y_0) is shown in panel B. Here we see that both variables increase and
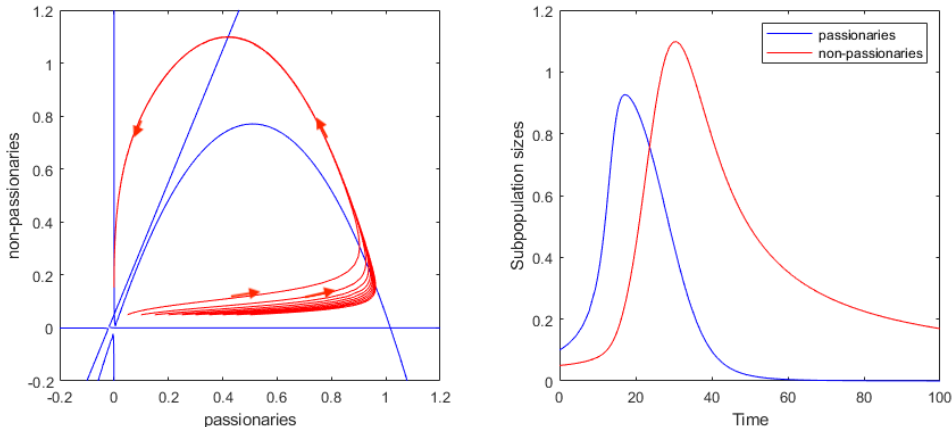
Figure 2: Illustration of the excitable dynamics observed in the system (6). Panel A: nullclines $\dot{x} = 0$ and $\dot{y} = 0$ are shown in blue and a set of phase trajectories with starting points $x = 0.05, 0.1, ..., 0.5$ and $y = y_0$ are shown in red. Panel B: time evolution of both variables, x (blue line) and y (red line) from the initial condition $x = 0.1$, $y = y_0$. Parameter values: $\alpha = 0.02$, $y_0 = 0.05$, $\beta_1 = -1/3$, $\beta_2 = 2.5$, $\gamma = 0.1$.

then decrease over time. We note a relatively fast dynamics of variable x (passionaries) with the duration of the spike being about 60 time unites. We also note a slow relaxation of variable y (the rest of population) which gets back to its equilibrium value with relaxation time of about 100 time units.

In order to scale the model time units to real time we take into account that according to Gumilev [8] the duration of passionary spike is about 900 years which should correspond to 60 time units in the model. Thus one model time unit corresponds to 15 years. Furthermore, according to Gumilev [8] the fraction of passionaries can only be up to 5-7% of the entire population. For the set of parameter values used to produce Fig. 2, both variables have values roughly in the range (0,1). If we consider variable x as representing 1% of y, the total number of nonpassionaries, then at the top of the spike (which takes place at $t \approx 15$ and where $x \approx 1$ and $y \approx 0.2$) the passionaries constitute about 5% of the entire population. In other words, $x = 1$ corresponds, e.g., to the absolute value of $K = 10,000$ passionaries, while $y = 1$ corresponds to $100K = 1,000,000$ nonpassionaries. One can certainly take other values of K. Note also that on the time interval $(20, 30)$ of the most rapid growth of nonpassionaries (constituting the main part of the population) their amount doubles. That corresponds to doubling time $\frac{10 \cdot 900}{60} = 150$ years which is roughly in line with observations of the maximal growth rate of human populations.

For the dynamics illustrated by Figure 2 it is essential that $\beta_1 < 0$ and $\beta_2 > 0$, that is, passionaries are suppressed by the rest of the population while their own impact to non-passionaries is positive. It appears that such relationships between passionaries and non-passionaries is not the only one allowing excitable dynamics. An alternative case when $\beta_1 > 0$ and $\beta_2 < 0$, that is, passionaries are activated by non-passionaries which are in turn suppressed by the passionaries can also result in the exciatable dynamics. This scenario is illustrated in Figure 3 which similarly to the Figure 2 shows the dynamics of the system (6) but with swapped signs of the parameters β_1 and β_2 and with $y_0 = 1$ (rather than $y_0 = 0.05$ in Figure 2). Panel A shows null-clines of the system and typical phase trajectories obtained from the over-threshold perturbation of the steady equilibrium $(x_2, y_2) = (0, y_0)$. Perturbation is made by an increase of the x-value over the threshold, $\alpha = 0.02$. Time dependence of the variables x and y for one of the phase trajectories is shown on panel B. Now we see that x and y change in opposite directions: initially x is increasing (for $t < 28$) and y is decreasing (for $t < 44$) and later both variables inverse their rate of change. Furthermore, here $y_0 = 1$ and the entire dynamics can be seen as change in fraction of passionaries over time for the population of a roughly constant size. Similarly to the case shown in Fig. 2, model time unit corresponds to 15 years.
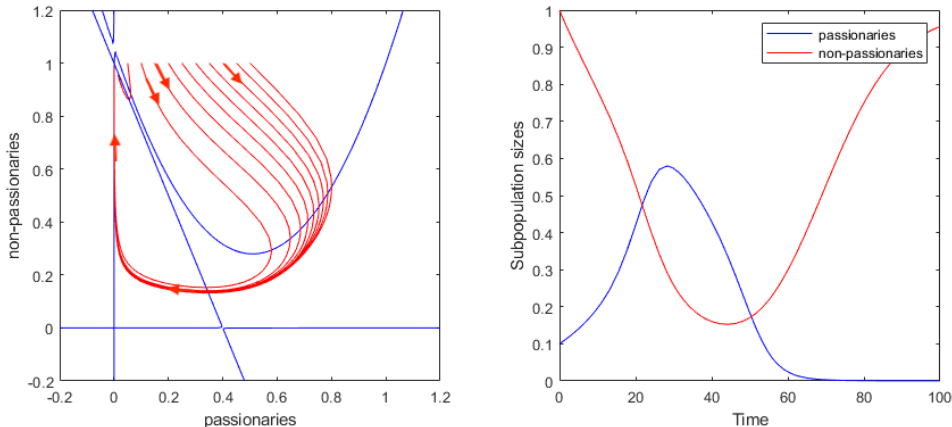
5

Figure 3: Illustration of the excitable dynamics in the system (6). Panel A: nullclines $\dot{x} = 0$ and $\dot{y} = 0$ are shown in blue and a set of phase trajectories with starting points $x_0 = 0.05, 0.1, ..., 0.5$ and y_0 are shown in red. Panel B: time evolution of both variables, x (blue line) and y (red line) from the initial condition $x = 0.1$, $y = y_0$. Parameter values: $\alpha = 0.02$, $y_0 = 1$, $\beta_1 = 1/3$, $\beta_2 = -2.5$, $\gamma = 0.1$.

There is an important difference between the dynamics shown in Figures 2 and 3. In Figure 2 the spike in variable x is followed by the spike in the variable y, that is, an increase in number of passionaries is followed by the increase of the size of remaining population. As for the dynamics shown in Figure 3 we notice that the increase in number of passionaries is followed by the decrease of the size of remaining population. We know that an increase in number of pasionaries results in the expansion of the polity and correspondingly to the growth of the population. Hence the dynamics shown in Figure 2 looks natural if the variable y represents harmonious people. However if the variable y is associated with subpassionaries then the dynamics in Figure 3 is not impossible as subpassionaries may be suppressed by the passionaries. Up to now the variable y was considered as including both, harmonious people and subpassionaries. In order to consider their dynamics separately we will modify our model by allocating variables to each of these two subpopulations.

3   Three-Variable Model

Gumilev in his theory of ethnogenesis considers three types of individuals who constitute ethnos and whose behaviour has an impact on the ethnogenetic process. To follow this concept we extend the two-variable model described by the system (6) by including extra variable z, so that the variables, x, y and z, represent the sizes of subpopulations of passionaries (x), harmonious people (y) and subpassionaries (z). Furthermore, we will presume that the dynamics of subpassionaries is similar to that of passionaries that is, their rate of change has quadratic dependence on their own sizes. However passionaries and subpassionaries differ by their relationships with harmonious people and each others. So, our three-variable system can be represented as the following:

$$\begin{cases} \dot{x} = \gamma_1 x[(1 - x)(x - \alpha_1) + \beta_{12}(y - y_0) + \beta_{13}(z - z_0)]; \\ \dot{y} = \gamma_2 y(y_0 - y + \beta_{21} x + \beta_{23}(z - z_0)); \\ \dot{z} = \gamma_3 z[(z_0 - z)(z - \alpha_2) + \beta_{31} x + \beta_{32}(y - y_0)] \end{cases} \quad (7)$$

with the initial condition $x(0), y(0), z(0) > 0$. Since its right-hand part is locally Lipschitz, the system (7) admits the unique local solution [19, Theorem 2.2.]. It looks that in general it can be extended to the unique bounded solution on the infinite horizon $[0, \infty)$.

Excitable dynamics can be observed in the system (7) under different kinds of interactions between the variables. In general, the steady states of the system (7) with $x = 0$ are as follows:

- $(x_1, y_1, z_1) = (0, 0, 0)$;

6

- $(x_2, y_2, z_2) = (0, y_0 - \beta_{23}z_0, 0)$;

- $(x_{3,4}, y_{3,4}, z_{3,4}) = (0, y_{3,4}, z_{3,4})$, where $y_{3,4}$ and $z_{3,4}$ are the two solutions to equations

$$\begin{cases} y_0 - y + \beta_{23}(z - z_0) = 0; \\ (z_0 - z)(z - \alpha_2) + \beta_{32}(y - y_0) = 0. \end{cases}$$

- $(x_{5,6}, y_{5,6}, z_{5,6}) = (0, 0, z_{5,6})$, where $z_{5,6}$ are the two solutions to equation

$$(z_0 - z)(z - \alpha_2) - \beta_{32}y_0 = 0.$$

In the case illustrated in Fig. 4, passionaries are suppressed by harmonious people ($\beta_{12} < 0$) and promoted by subpassionaries ($\beta_{13} > 0$); harmonious people are promoted by passionaries ($\beta_{21} > 0$) as well as by subpassionaries ($\beta_{23} > 0$); subpassionaries are promoted by passionaries ($\beta_{31} > 0$) and do not depend on harmonious people ($\beta_{32} = 0$). For the set of parameter values used in the simulation shown in Fig. 4, there are eight real-valued steady states, with seven among them that have non-negative coordinates. All the steady states with non-zero component x are unstable. Among the six steady states enlisted above, $(x_1, y_1, z_1) = (0, 0, 0)$, $(x_3, y_3, z_3) = (0, 0.064, 0.11)$, $(x_5, y_5, z_5) = (0, 0, 0.22)$ and $(x_6, y_6, z_6) = (0, 0, 0.11)$ are unstable, and the steady states $(x_2, y_2, z_2) = (0, 0.053, 0)$ and $(x_4, y_4, z_4) = (0, 0.075, 0.22)$ are stable. In Fig. 4 the stable steady states are shown with big spots, and the unstable steady state $(x_3, y_3, z_3) = (0, 0.064, 0.11)$ between them is indicated as the short line.
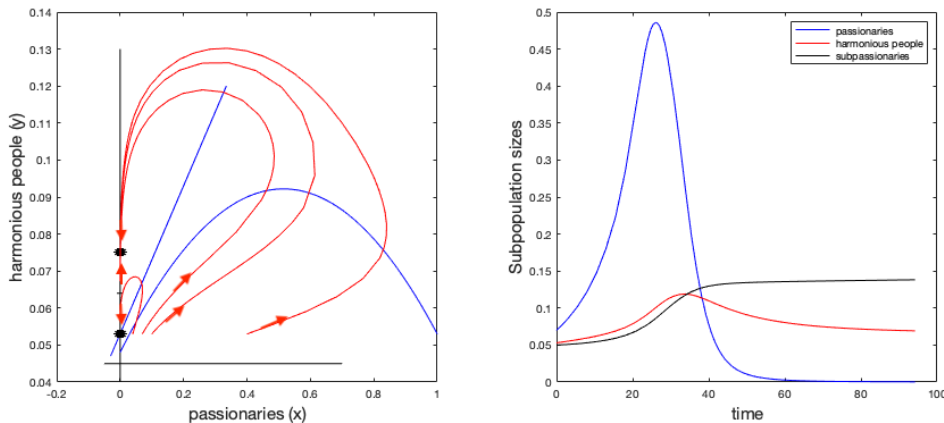

Figure 4: Illustration of the excitable dynamics in the system (7). Panel A: nullclines $\dot{x} = 0$ and $\dot{y} = 0$ at $z = z_0$ are shown in blue and a set of phase trajectories with starting points $x(0) = 0.04, 0.07, 0.1, 0.4$ and $y(0) = 0.053$, $z(0) = 0.05$ are shown in red. Panel B: time evolution of all three variables, x (blue line), y (red line) and z (black line) from the initial condition $x(0) = 0.07$, $y(0) = 0.053$, $z(0) = 0.05$. Parameter values: $\alpha_1 = 0.03$, $\alpha_2 = 0.11$, $y_0 = 0.075$, $z_0 = 0.22$, $\beta_{12} = -6$, $\beta_{13} = 0.6$, $\beta_{21} = 0.2$, $\beta_{23} = 0.1$, $\beta_{31} = 0.5$, $\beta_{32} = 0$, $\gamma_1 = 1$, $\gamma_2 = 0.7$, $\gamma_3 = 0.2$.

The excitation appears, starting in the neighbourhood of the stable point (x_2, y_2, z_2) $= (0, 0.053, 0)$ which is shown as the lower spot on the vertical axis. We assigned the initial values $z(0) = 0.05$ (to give a push from the 'cemetery' $z = 0$), $y(0) = 0.053$; $x(0)$ varies from 0.04 to 0.4. If the initial push $x(0)$ is below or slightly above the threshold α_1, the system quickly returns back to the state (x_2, y_2, z_2). But larger (still small enough) initial perturbation results in the excitation leading to the second stable point $(x_4, y_4, z_4) = (0, 0.075, 0.22)$ shown as the upper spot on the vertical axis. Depending on the value of $x(0)$, the trajectory approaches the limit (x_4, y_4, z_4) either from below or from above. Even a small over-threshold perturbation $x(0) = 0.07 > \alpha_1$ grows up to around $x = 0.5$ before it relaxes back to $\lim_{t \to \infty} x(t) = 0$. Qualitatively, the picture is similar to that presented in Fig. 2. Again, one model time unit corresponds to 15 years.
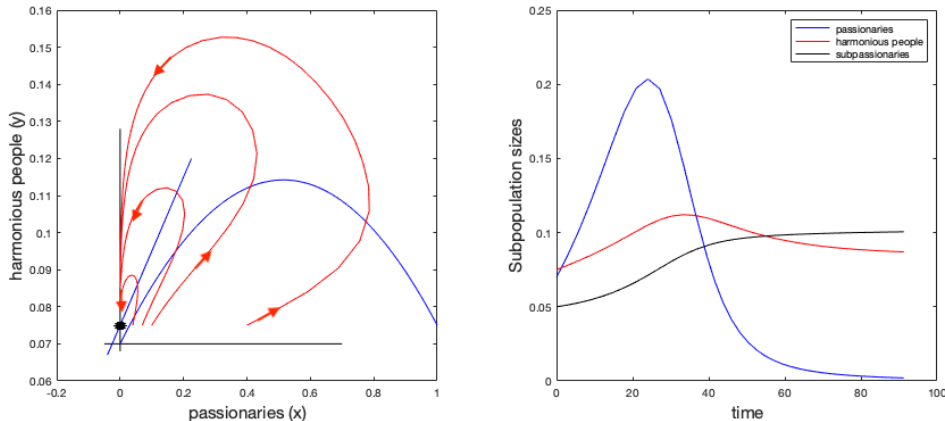
7

Figure 5: Illustration of the excitable dynamics in the system (7). Panel A: nullclines $\dot{x} = 0$ and $\dot{y} = 0$ at $z = z_0$ are shown in blue and a set of phase trajectories with starting points $x(0) = 0.04, 0.07, 0.1, 0.4$ and $y(0) = 0.075$, $z(0) = 0.05$ are shown in red. Panel B: time evolution of all three variables, x (blue line), y (red line) and z (black line) from the initial condition $x(0) = 0.07$, $y(0) = 0.075$, $z(0) = 0.05$. Parameter values: $\alpha_1 = 0.03$, $\alpha_2 = 0.11$, $y_0 = 0.075$, $z_0 = 0.$, $\beta_{12} = -6$, $\beta_{13} = 0.6$, $\beta_{21} = 0.2$, $\beta_{23} = 0.1$, $\beta_{31} = 0.5$, $\beta_{32} = 0$, $\gamma_1 = 1$, $\gamma_2 = 0.7$, $\gamma_3 = 0.2$.

As a special case, one can put $z_0 = 0$ leaving the other parameters the same. For this set of parameter values, used in the simulation shown in Fig. 5, there is only one stable steady state $(x, y, z) = (0, 0.075, 0)$: all three previous equilibria $(x_{2,3,4}, y_{2,3,4}, z_{2,3,4})$ now coincide. The system again exhibits excitable kinetics: over-threshold perturbation of x ($x > \alpha_1$) grows up to around $x = 0.2$ before it relaxes back to equilibrium.

An alternative dynamics for the system (7) is shown in Fig 6. Here the interactions between the variables is slightly different from those used for the dynamics illustrated in Fig 4. The difference is that harmonious people are suppressed (rather than promoted) by subpassionaries ($\beta_{23} < 0$) and subpassionaries are promoted (rather than suppressed) by passionaries ($\beta_{31} < 0$). For the set of parameter values used in the simulation shown in Fig. 6 there are two stable steady states $(x_2, y_2, z_2) = (0, 0.12, 0)$ and $(x_4, y_4, z_4) = (0, y_0, z_0)$: the enumeration is in accordance with the expressions below equation (7). The system at the steady state (x_4, y_4, z_4) exhibits excitable kinetics: over-threshold perturbation of x ($x > \alpha_1$) grows up to around $x = 0.7$ before it relaxes back to the equilibrium (x_4, y_4, z_4). As we have two stable states, the relaxation can bring the system to another steady state (x_2, y_2, z_2), and this is observed in the system with slightly different set of parameter values. Qualitatively, the dynamics illustrated in Fig 6 is similar to that presented in Fig. 3.

One can see that in Fig. 6 the number of subpassionaries dramatically decreases before going back to the equilibrium. This perhaps does not often occur in reality. The dynamic in Fig. 5 looks more reasonable. But the growth of the passionaries subpopulation (from 0.07 to 0.2) is not as impressive as in Fig. 4 (from 0.07 to 0.49). Therefore, in further simulations, we take the parameter values from the latter case (Fig. 4). If $\beta_{12} \leq 0$, $\beta_{32} \leq 0$ the existence of the unique bounded solution to the system (7) will follow from the investigation of the stochastic version of the model: see Proposition 4.1 and its proof, especially, Remark 7.2.

4   Ethnogenesis in Noisy Environment

In order to study the impact of noise on the ethnogenetic process we will modify the three-variable model by adding extra (stochastic) terms to the system (7). To justify the modification which we are about to impose, let us consider the following change of variables:

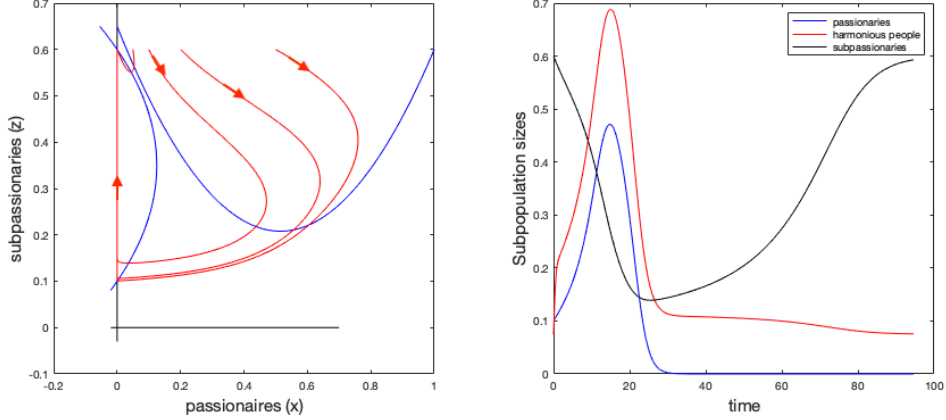$$v_1 = \ln x, \qquad v_2 = \ln y, \qquad v_3 = \ln z. \tag{8}$$

8

Figure 6: Illustration of the excitable dynamics in the system (7). Panel A: nullclines $\dot{x} = 0$ and $\dot{z} = 0$ at $y = y_0$ are shown in blue and a set of phase trajectories with starting points $x(0) = 0.05, 0.1, 0.2, 0.5$ and $y(0) = y_0, z(0) = z_0$ are shown in red. Panel B: time evolution of all three variables, x (blue line), y (red line) and z (black line) from the initial condition $x(0) = 0.1$, $y(0) = y_0, z(0) = z_0$. Parameter values: $\alpha_1 = 0.03$, $\alpha_2 = 0.1$, $y_0 = 0.075$, $z_0 = 0.6$, $\beta_{12} = -0.06$, $\beta_{13} = 0.6$, $\beta_{21} = 1.25$, $\beta_{23} = -0.075$, $\beta_{31} = -0.5$, $\beta_{32} = 0$, $\gamma_1 = 2$, $\gamma_2 = 20$, $\gamma_3 = 0.6$.

With these variables the equations (7) transform into

$$
\begin{cases}
\dot{v_1} = \gamma_1[(1 - e^{v_1})(e^{v_1} - \alpha_1) + \beta_{12}(e^{v_2} - y_0) + \beta_{13}(e^{v_3} - z_0)]; \\
\dot{v_2} = \gamma_2[y_0 - e^{v_2} + \beta_{21}e^{v_1} + \beta_{23}(e^{v_3} - z_0)]; \\
\dot{v_3} = \gamma_3[(z_0 - e^{v_3})(e^{v_3} - \alpha_2) + \beta_{31}e^{v_1} + \beta_{32}(e^{v_2} - y_0)],
\end{cases}
\tag{9}
$$

with the initial conditions $v_1(0) = \ln x(0)$, $v_2(0) = \ln y(0)$, $v_3(0) = z(0)$. Note that v_1, v_2 and v_3 may be negative and the initial conditions $x(0), y(0), z(0) > 0$ are assumed to be fixed.

The natural way to define the stochastic version is to introduce stochastic differential equations

$$
\begin{cases}
dV_1 = \gamma_1[(1 - e^{V_1})(e^{V_1} - \alpha_1) + \beta_{12}(e^{V_2} - y_0) + \beta_{13}(e^{V_3} - z_0)]dt + \sigma_1 dW_1; \\
dV_2 = \gamma_2[y_0 - e^{V_2} + \beta_{21}e^{V_1} + \beta_{23}(e^{V_3} - z_0)]dt + \sigma_2 dW_2; \\
dV_3 = \gamma_3[(z_0 - e^{V_3})(e^{V_3} - \alpha_2) + \beta_{31}e^{V_1} + \beta_{32}(e^{V_2} - y_0)]dt + \sigma_3 dW_3; \\
V_1(0) = v_1(0), \qquad V_2(0) = v_2(0), \qquad V_3(0) = v_3(0),
\end{cases}
\tag{10}
$$

which we understand in the sense of the Ito stochastic calculus [14]. Here W_1, W_2 and W_3 are mutually independent standard Brownian motions on the complete filtered probability space $(\Omega, \mathcal{F}, (\mathcal{F}_t)_{t \geq 0}, P)$, and $\sigma_1, \sigma_2, \sigma_3 > 0$. After that,

$$
X = e^{V_1}, \qquad Y = e^{V_2}, \qquad Z = e^{V_3}
$$

will be the random processes representing the sizes of the subpopulations of passionaries, harmonious people and subpassionaries respectively.

According to Proposition 4.1, the random processes (V_1, V_2, V_3) and (X, Y, Z) do exist. Obviously, $X(t), Y(t), Z(t) > 0$, but one cannot say much about the densities of the random variables $X(t), Y(t)$ and $Z(t)$. If $X(t) = x$, $Y(t) = y$ and $Z(t) = z$, then at the end of a small time interval $[t, t + \Delta]$, roughly speaking, we have

$$
X(t + \Delta) = (x + \Delta x)e^{\sigma_1 \Delta W_1}, \quad Y(t + \Delta) = (y + \Delta y)e^{\sigma_2 \Delta W_2}, \quad Z(t + \Delta) = (z + \Delta z)e^{\sigma_3 \Delta W_3}.
$$

Here $(\Delta x, \Delta y, \Delta z)$ are the (deterministic) increments according to the differential equations (7), and $\sigma_i \Delta W_i \sim N(0, \sigma_i^2 \Delta)$. Thus, $X(t + \Delta), Y(t + \Delta)$ and $Z(t + \Delta)$ have approximately log-normal (sometimes called Galton) distributions with densities

$$
f_1(u) = \frac{1}{u\sigma_1\sqrt{2\pi\Delta}}e^{-\frac{(\ln u - \ln(x + \Delta x))^2}{2\sigma_1^2\Delta}}, \quad u > 0; \quad f_2(u) = \frac{1}{u\sigma_2\sqrt{2\pi\Delta}}e^{-\frac{(\ln u - \ln(y + \Delta y))^2}{2\sigma_2^2\Delta}}, \quad u > 0;
$$

and $f_3(u) = \dfrac{1}{u\sigma_3\sqrt{2\pi\Delta}} e^{-\frac{(\ln u - \ln(z+\Delta z))^2}{2\sigma_3^2\Delta}}$, $\quad u > 0$ correspondingly.

Note that X, Y and Z satisfy stochastic differential equations

$$
\begin{cases}
dX = \gamma_1 X[(1-X)(X-\alpha_1) + \beta_{12}(Y-y_0) + \beta_{13}(Z-z_0) + \frac{\sigma_1^2}{2}]dt + \sigma_1 X dW_1; \\
dY = \gamma_2 Y[y_0 - Y + \beta_{21}X + \beta_{23}(Z-z_0) + \frac{\sigma_2^2}{2}]dt + \sigma_2 Y dW_2; \\
dZ = \gamma_3 Z[(z_0-Z)(Z-\alpha_2) + \beta_{31}X + \beta_{32}(Y-y_0) + \frac{\sigma_3^2}{2}]dt + \sigma_3 Z dW_3; \\
X(0) = x(0), \qquad Y(0) = y(0), \qquad Z(0) = z(0).
\end{cases}
\tag{11}
$$

Derivation of (11) can be found in [14] where it is stated as Theorem 4.2.1. Here and below, capital letters denote random variables and processes.

In what follows, all the coefficients in (7), (9), (10) and (11) are assumed to be positive apart from $\beta_{12} \leq 0$ and $\beta_{32} \leq 0$.

Proposition 4.1. *Stochastic differential equations (10) (and hence (11)) have a unique strong continuous solution on the time horizon* $[0, \infty)$.

The proof is presented in the Appendix. Note that the standard theory of stochastic differential equations is developed only for linear equations. In the recent works (see, e.g., [26] and references therein), theorems similar to Proposition 4.1 were proved for specific quadratic equations describing population dynamics, using the Lyapunov function. Equations (11) are of the third order and require special reasoning. Proposition 4.1 implies that, under positive initial conditions, the ordinary differential equations (7) (and hence (6)) have a unique solution such that $x(t), y(t), z(t) > 0$ for all $t \geq 0$: see Remark 7.2.
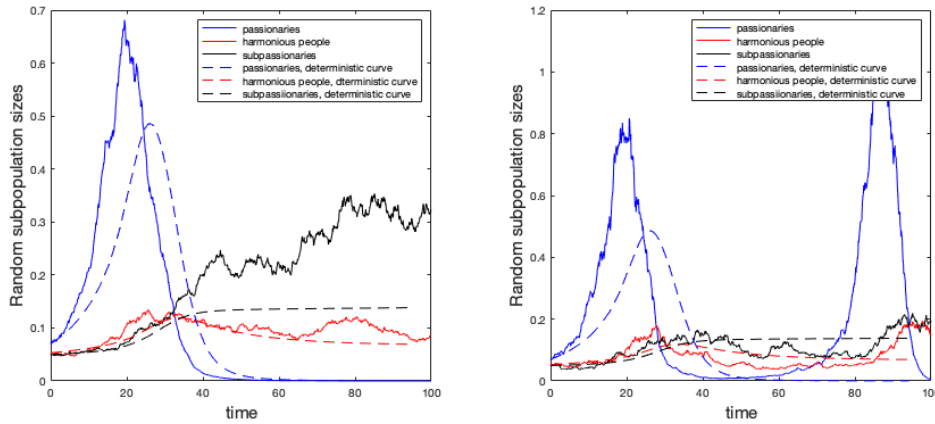

Figure 7: Stochastic dynamics of the ethnogenesis: examples of the solution to stochastic differential equations (11). Parameter values: $\alpha_1 = 0.03$, $\alpha_2 = 0.11$, $y_0 = 0.075$, $z_0 = 0.22$, $\beta_{12} = -6$, $\beta_{13} = 0.6$, $\beta_{21} = 0.2$, $\beta_{23} = 0.1$, $\beta_{31} = 0.5$, $\beta_{32} = 0$, $\gamma_1 = 1$, $\gamma_2 = 0.7$, $\gamma_3 = 0.2$, Initial conditions: $X(0) = 0.07$, $Y(0) = 0.053$, $Z(0) = 0.05$. Panel A: $\sigma_1 = \sigma_2 = \sigma_3 = 0.05$. Panel B: $\sigma_1 = \sigma_2 = \sigma_3 = 0.1$.

Examples of the stochastic dynamics exhibited in the system (11) are shown in Fig. 7. The values of model parameters used for this illustration are identical to those in Fig. 4. The amplitude of noise in Panel B is twice higher than in Panel A. Solid lines in both panels show the stochastic dynamics for three subgroups composing the population. For comparison, we also provide the deterministic curves which are represented by dashed lines (note, that they are identical to the lines shown in Fig. 4, panel B). It is evident that the stochastic dynamics is significantly different from the deterministic one. One can see from Panel A that the accumulation of noise results in a much higher bust in the level of passionaries: the amplitude of the bust in the stochastic case is about 0.7 against 0.5 in the deterministic one. Also in Panel A we see that the noise causes significant change in the level of subpassionaries: at t=100 this level in stochastic case is over 0.3

while it should be about 0.13 in the deterministic case. The impact of noise is even more evident from Panel B where the amplitude of noise is twice higher than in Panel A. We can see that the increase in the level of noise not only increases the discrepancy with the deterministic case (the amplitude of bust in Panel B is over 0.8) but also results in the occurrence of a new bust. While the first bust in Panel B was initiated manually, the second bust appears due to the stochastic effects in the system. This observation leads us to the conclusion that the ethnogenesis can be initiated by the noise in the environment surrounding the population.

5   Interaction of Ethnogenetic Processes

We conclude our study with modelling the interaction between two ethnoses, following the same ethnogenetic processes, which however are shifted over time. The (random) sizes of subpopulations of passionaries, harmonious people and subpassionaries for the first ethnos are denoted as X_1, Y_1 and Z_1, while for the second ethnos as X_2, Y_2 and Z_2. We assume that, being isolated, the ethnoses are identical, described by the stochastic differential equations like (11), but influenced by six mutually independent Brownian motions $W_1, W_2, \ldots, W_6$. We introduce the time lag between two ethnogenetic processes, such that the first one starts at $T = 0$, the second ethnos appears T_1 time units later than the first one, and communication begins T_2 time units later, at the moment $T_1 + T_2$. For simplicity, we also assume that communication is only among the passionaries, and they suppress each other.

Therefore, we investigate the following system of six stochastic differential equations

$$
\begin{cases}
dX_1 = \gamma_1 X_1[(1-X_1)(X_1-\alpha_1) + \beta_{12}(Y_1-y_0) + \beta_{13}(Z_1-z_0) + \frac{\sigma_1^2}{2} \\
\qquad -c_1 \mathbb{I}\{t \geq T_1 + T_2\}X_2]dt + \sigma_1 X_1 dW_1; \\
dY_1 = \gamma_2 Y_1[y_0 - Y_1 + \beta_{21}X_1 + \beta_{23}(Z_1-z_0) + \frac{\sigma_2^2}{2}]dt + \sigma_2 Y_1 dW_2; \\
dZ_1 = \gamma_3 Z_1[(z_0-Z_1)(Z_1-\alpha_2) + \beta_{31}X_1 + \beta_{32}(Y_1-y_0) + \frac{\sigma_3^2}{2}]dt + \sigma_3 Z_1 dW_3; \\
X_1(0) = x(0), \qquad Y_1(0) = y(0), \qquad Z_1(0) = z(0); \\[2mm]
dX_2 = \mathbb{I}\{t \geq T_1\}\Big\{\gamma_1 X_2[(1-X_2)(X_2-\alpha_1) + \beta_{12}(Y_2-y_0) + \beta_{13}(Z_2-z_0) + \frac{\sigma_1^2}{2} \\
\qquad -c_2 \mathbb{I}\{t \geq T_1 + T_2\}X_1]dt + \sigma_1 X_2 dW_4 \Big\}; \\
dY_2 = \mathbb{I}\{t \geq T_1\}\Big\{\gamma_2 Y_2[y_0 - Y_2 + \beta_{21}X_2 + \beta_{23}(Z_2-z_0) + \frac{\sigma_2^2}{2}]dt + \sigma_2 Y_2 dW_5 \Big\}; \\
dZ_2 = \mathbb{I}\{t \geq T_1\}\Big\{\gamma_3 Z_2[(z_0-Z_2)(Z_2-\alpha_2) + \beta_{31}X_2 + \beta_{32}(Y_2-y_0) + \frac{\sigma_3^2}{2}]dt + \sigma_3 W_6 \Big\}; \\
X_2(0) = X_2(T_1) = x(0), \qquad Y_2(0) = Y_2(T_1) = y(0), \qquad Z_2(0) = Z_2(T_1) = z(0).
\end{cases}
\tag{12}
$$

The meaning of all the parameters is the same as in the previous models (i.e. model (11)). Two new parameters ($c_1, c_2 > 0$) define the strength of suppressive interactions between passionaries in the two ethnic groups. This system of stochastic differential equations has a unique strong continuous solution on the time horizon $[0, \infty)$. The proof of this statement is similar to the proof of Proposition 4.1.

Two examples of dynamics in the interacting ethnoses, described by the system (12), is given in Fig.8. Only the bust dynamics exhibited by the passionaries in both ethnoses is shown on this figure, with the solid lines showing stochastic dynamics, dashed - deterministic ($\sigma_1 = \sigma_2 = \sigma_3 = 0$) and dotted - the deterministic dynamics in the case of non-interacting ethnoses ($c_1 = c_2 = 0$). Dotted lines have identical shapes and this indicates that the two ethnogenetic processes, in the absence of noise and interaction between the ethnoses, are identical. While the dashed blue line is almost identical to the dotted blue line, the dashed red line is considerably lower than the dotted red line, and this indicates that, in the absence of noise, the younger ethnos (dashed red line) is suppressed by the older ethnos (dashed blue line). Finally we note that the solid blue line in Panel A is higher than the dashed blue line, while the solid red line is lower than the dashed red line. This observation illustrated the impact of the noise to the dynamics of the interacting ethnoses, which in this particular case results in the amplification of the suppression of the younger ethnos
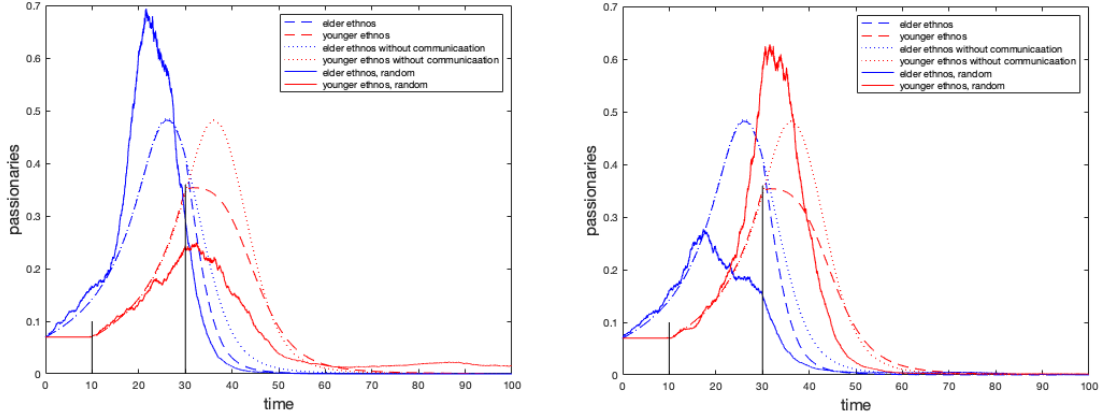
Figure 8: Stochastic dynamics of communicating ethnoses. Parameter values: $\alpha_1 = 0.03$, $\alpha_2 = 0.11$, $y_0 = 0.075$, $z_0 = 0.22$, $\beta_{12} = -6$, $\beta_{13} = 0.6$, $\beta_{21} = 0.2$, $\beta_{23} = 0.1$, $\beta_{31} = 0.5$, $\beta_{32} = 0$, $\gamma_1 = 1$, $\gamma_2 = 0.7$, $\gamma_3 = 0.2$, $c_1 = c_2 = 0.22$, $\sigma_1 = \sigma_2 = \sigma_3 = 0.04$. The black vertical lines show the moment of birth of the younger ethnos and the moment when the communication begins. Initial conditions: $X(0) = 0.07$, $Y(0) = 0.053$, $Z(0) = 0.05$.

by the older one. Looking at the shapes of the solid and dashed lines on Panel B we come to the conclusion that the noise can also result in the suppression of the older ethnos by the younger one. Comparing dynamics presented in Panels A and B we note that the dynamics exhibited by two interacting ethnoses is greatly affected by the noise, although, as numerous simulations confirm, the scenario from Panel A is more likely to take place.

6   Summary and Discussion

In this work we have presented the mathematical model of ethnogenesis which we have developed on the basis of the paradigm of "passionary tension" introduced by Gumilev [9]. According to Gumilev, passionary tension can occur in certain polities as a result of formation and growth of a subgroup of positively motivated people, whom Gumilev called "passionaries". One of the main points made by Gumilev is that the measure of passionary tension in the polity is given by its size, i.e. the size of population or territory. As the quantitative data on the territorial expansion and collapse of past civilizations are much better known than on their population sizes, it makes sense to use the size of area taken by a polity as a measure of the passionary tension in this polity.

The model we have presented here is based on the consideration of the internal structure of the polity with the dynamics of this structure described by ordinary differential equations. The main point about the polity's internal structure is that there is a subgroup of people, namely, passionaries, and the size of this subgroup gives a measure of the passionary tension in the polity, which in turn can be considered as the measure of the size of territory occupied by the polity. This approach allows to consider the interaction of the given polity with its neighbours indirectly: the polity's geopolitical success is proportional to the number of passionaries in it.

The main feature of the model we have presented here is that it produces the excitable dynamics in the structure of the evolving polity. That is, when the polity is in equilibrium (in homoeostatic state) there are no passionaries in it. However, if there appear a small number of passionaries, this number grows up to considerable level and then declines back to zero. Thus, formation of busts, describing the raise and fall of civilizations, is considered here as an excitation process. Using different versions of the model we have performed the following studies:

- In the two-variable model given by (6) we explored the types of interactions between the passionaries and the rest of the population resulting in the excitable kinetics. Two types of such interactions are illustrated in Figures 2 and 3.

12

- In the three-variable model given by (7) we explored the types of interactions between three groups allowing to observe the excitable kinetics. Three types of such interactions are illustrated in Figures 4, 5 and 6.

- In the stochastic model given by (11) we have found that the noise, when imposed into the model equations, tends to amplify and results in significant variations in the amplitude of the bust in the system (see Figure 7). One can conclude that such noise probably adds to the variation of the territorial size and duration of life of different civilizations.

- In the model of interacting polities given by (12) we studied the interaction of the polities of different age undergoing ethnogenesis. We found that if they interact in a way that passionaries from one polity suppress the passionaries from the other, then the older polity will be more successful, if the success is measured by the number of passionaries in the polity. However, this is not necessarily the case when we impose the noise (see Figure 8).

It is evident that most of recent theoretical studies of ethnogenesis are focused on civilizations/polities which evolve under no (or negligible) influence of their neighbours. The core statements in Gumilev's theory are about polities which grow into civilizations despite external impacts from neighbouring polities. Also, Gumilev defines civilization as meta-ethnic polity which is formed in the course of expansion of a core ethnic group and which he calls "super-ethnos". The main focus in our study is on the dynamics of an isolated polity or the polity under negligible external impact. The presented model is probably the simplest model which reproduces boom-and-bust dynamics and gives it a fairly simple explanation in terms of excitability.

We scaled our model to fit to the lifespan of civilizations which, according to Gumilev, varies between twelve and fifteen centuries. Other researchers who studied the cyclic dynamics of large polities (i.e. empires) have concluded that their lifespan can be considerably shorter [18]. We believe that our model can be fitted and applied to such short-living polities too. An interesting problem lies on the other side of time scale, that is, whether our model can make sense and be applied to the dynamics of global civilization. Today there is no information about whether the global civilization has the boom-and-bust dynamics, and we can speculate that the time scale for such dynamics would probably be 100,000-1,000,000 years, not 1,500 as in the case of civilizations, considered by Gumilev.

The most intriguing questions concerning Gumilev's theory are "What is passionarity?" and "How does it evolve on a populational level?". Peter Turchin has explained, at least verbally, an increase of asabiya on frontiers [24]. As Ibn Khaldun's concepts of asabiya is similar to Gumilev's concept of passionarity one could use Turchin's verbal explanations for developing a mathematical model to reproduce the selection of passionaries on frontiers versus the selection of harmonious people in inner lands. Mathematical studies of development of other psycho-ethic characterises, such as altruism, on populational level are known [2] and can be used as sample studies. Another important question is how universal is the impact of passionarity on the dynamics of polities across different societies. Gumilev stated his theory as universal and valid across all times and continents. However, recent studies indicate that psychological states of people, such as human reflection, is different between Western and Eastern societies [12] and thus the impact of passionarity can vary across different societies.

The presented model can be extended in various ways for further studies. One of such studies can focus on the interaction of polities under a range of different assumptions about the ways these polities interact. Another direction for future research is to extend the model in order to fit it to available observation data.

7 Appendix

Proof of Proposition 4.1. Similarly to Fig. 4, panel A, we present the nullclines $\dot{x} = 0$ and $\dot{z} = 0$ at $y = 0$ in Fig. 9, panel A. Fix a point $(a, c) \in \mathbb{R}_+ \times \mathbb{R}_+$ such that

$$(1 - a)(a - \alpha_1) - \beta_{12}y_0 + \beta_{13}(z - z_0) < 0 \qquad \text{for all } z \leq c;$$
$$(z_0 - c)(c - \alpha_2) + \beta_{31}x - \beta_{32}y_0 < 0 \qquad \text{for all } x \leq a.$$

The half-open rectangle $(0, a] \times (0, c]$ is shown with the green lines. Clearly, it is always possible to increase simultaneously a and c, so we assume that $a, c > 1$, $0 < x(0) < a$ and $0 < z(0) < c$. Roughly speaking, the point (a, c) is outside the 'internal part' of both parabolas.

The similar picture in the variables (8) is given in Fig. 9, panel B: the images of the parabolas, shown with the blue lines, represent the nullclines $\dot{v}_1 = 0$ and $\dot{v}_3 = 0$ of equation (9) in the limiting case when $v_2 \to -\infty$.
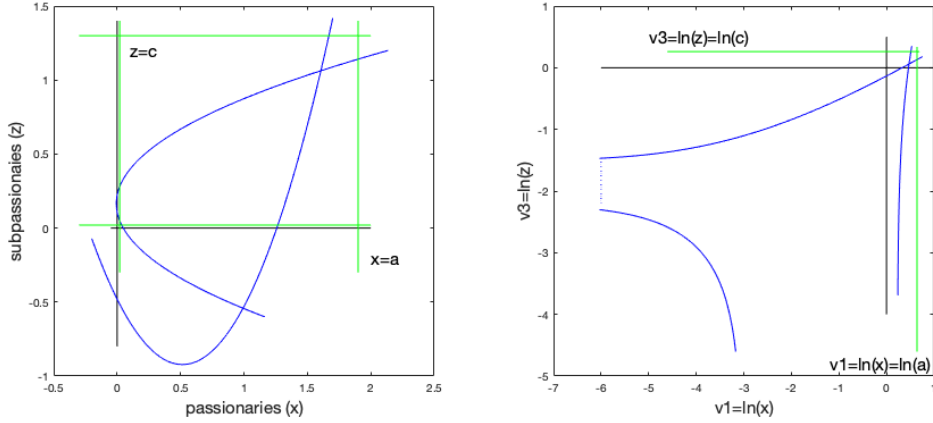

Figure 9: Panel A: nullclines $\dot{x} = 0$ and $\dot{z} = 0$ at $y = 0$ are shown in blue. Panel B: nullclines $\dot{v}_1 = 0$ and $\dot{v}_3 = 0$ at $v_2 \to -\infty$ are shown in blue. The dotted blue line corresponds to the part of the parabola $\dot{z} = 0$ with negative values of x. Parameter values: $\alpha_1 = 0.03$, $\alpha_2 = 0.11$, $y_0 = 0.075$, $z_0 = 0.22$, $\beta_{12} = -6$, $\beta_{13} = 0.6$, $\beta_{21} = 0.2$, $\beta_{23} = 0.1$, $\beta_{31} = 0.5$, $\beta_{32} = 0$, $\gamma_1 = 1$, $\gamma_2 = 0.7$, $\gamma_3 = 0.2$.

In the space $\mathbb{R}^3$, consider the infinite closed prism Π defined by

$$-\infty < v_1 \leq \ln a, \qquad -\infty < v_2 \leq \ln b, \qquad -\infty < v_3 \leq \ln c,$$

where

$$b > y_0 + \beta_{21}a + \beta_{23}(c - z_0). \tag{13}$$

Without loss of generality, we assume that $y(0) < b$ and $b > 1$.

Remark 7.1. *For such a prism, we have the following.*

- *If $x = a$, then the square bracket in the first equation (7) is negative for all $z \leq c$ and all $y > 0$. (Recall that $\beta_{12} \leq 0$.) Therefore, if $v_1 = \ln a$, then the square bracket in the first equation (9) and (10) is negative for all $v_3 \leq \ln c$ and all $v_2 > -\infty$.*

- *Similarly, if $z = c$ then the square bracket in the third equation (7) is negative for all $x \leq a$ and all $y > 0$. (Recall that $\beta_{32} \leq 0$.) Therefore, if $v_3 = \ln c$, then the square bracket in the third equation (9) and (10) is negative for all $v_1 \leq \ln a$ and all $v_2 > -\infty$.*

- *If $y = b$, then the square bracket in the second equation (7) is negative for all $x \leq a$ and $z \leq c$. Therefore, if $v_2 = \ln b$, then the square bracket in the second equation (9) and (10) is negative for all $v_1 \leq \ln a$ and all $v_3 \leq \ln c$.*

Now we modify the equations (10) outside Π: if $(v_1, v_2, v_3) = m(\hat{v}_1, \hat{v}_2, \hat{v}_3)$ for some $m > 1$ with $(\hat{v}_1, \hat{v}_2, \hat{v}_3) \in \partial\Pi$, then we put

$$\begin{cases} f_1(v_1, v_2, v_3) := \gamma_1[(1 - e^{\hat{v}_1})(e^{\hat{v}_1} - \alpha_1) + \beta_{12}(e^{\hat{v}_2} - y_0) + \beta_{13}(e^{\hat{v}_3} - z_0)]; \\ f_2(v_1, v_2, v_3) := \gamma_2[y_0 - e^{\hat{v}_2} + \beta_{21}e^{\hat{v}_1} + \beta_{23}(e^{\hat{v}_3} - z_0)]dt; \\ f_3(v_1, v_2, v_3) := \gamma_3[(z_0 - e^{\hat{v}_3})(e^{\hat{v}_3} - \alpha_2) + \beta_{31}e^{\hat{v}_1} + \beta_{32}(e^{\hat{v}_2} - y_0)]dt \end{cases}$$

and introduce stochastic differential equations (further, SDEs)

$$\begin{cases} dV_1 = f_1(V_1, V_2, V_3)dt + \sigma_1 dW_1; \\ dV_2 = f_2(V_1, V_2, V_3)dt + \sigma_2 dW_2; \\ dV_3 = f_3(V_1, V_2, V_3)dt + \sigma_3 dW_3, \\ V_1(0) = v_1(0), \qquad V_2(0) = v_2(0), \qquad V_3(0) = v_3(0). \end{cases} \qquad (14)$$

They satisfy all the conditions which guarantee the existence of the unique continuous strong solution [4, Remark 14.21] or [14, Theorem 5.2.1]: all the functions f_1, f_2 and f_3 are bounded and Lipschitz in $\mathbb{R}^3$.

Remark 7.2. *If $\sigma_1 = \sigma_2 = \sigma_3 = 0$, we have just the system of ordinary differential equations which is uniquely solvable on the time horizon $[0, \infty)$ [19, Corollary 2.6.]. This solution $(v_1(t), v_2(t), v_3(t))$ can never leave the prism Π because on the boundary $\ln a$ for the component v_1 ($\ln b$ for v_2 and $\ln c$ for v_3) the derivative $\dot{v}_1$ is negative ($\dot{v}_2 < 0$ and $\dot{v}_3 < 0$ correspondingly): see Remark 7.1.*

Finally, within the prism Π, the vector $(v_1(t), v_2(t), v_3(t))$ satisfies differential equations (9) and the functions $x(t) := e^{v_1(t)}$, $y(t) := e^{v_2(t)}$ and $z := e^{v_3(t)}$ are well defined on the infinite horizon $[0, \infty)$, satisfy equations (7) and are strictly positive. As was noted below (7), these equations cannot have other solutions.

In the stochastic version with $\sigma_1, \sigma_2, \sigma_3 > 0$, the solution to SDE (14) can exit any one prism on a finite time interval. We need to define a sequence of increasing prisms $\{\Pi_i\}_{i=0}^{\infty}$ coming from a carefully selected sequence $\{(a_i, b_i, c_i)\}_{i=0}^{\infty}$. Namely, we require that, for a preliminarily fixed $k > 0$, the following condition is satisfied.

Condition 7.1. *For each $i > 0$ for all*

$$a_{i-1} \le x \le a_i, \qquad 0 < y \le b_i, \qquad 0 < z \le c_i$$
$$(or \qquad 0 < x \le a_i, \qquad b_{i-1} \le y \le b_i, \qquad 0 < z \le c_i$$
$$or \qquad 0 < x \le a_i, \qquad 0 < y \le b_i, \qquad c_{i-1} \le z \le c_i)$$

the square bracket in the first (second, third) equation (7) is negative and $a_i \ge a_{i-1}e^k$ ($b_i \ge b_{i-1}e^k$, $c_i \ge c_{i-1}e^k$ correspondingly). As the result, for all $(v_1, v_2, v_3) \in \Pi_i$ with $v_1 \in [\ln a_{i-1}, \ln a_i]$ (with $v_2 \in [\ln b_{i-1}, \ln b_i]$, $v_3 \in [\ln c_{i-1}, \ln c_i]$) the square bracket in the first (correspondingly, second, third) equation (9) and (10) is negative.

Additionally, $\ln a_i \ge \ln a_{i-1} + k$ ($\ln b_i \ge \ln b_{i-1} + k$, $\ln c_i \ge \ln c_{i-1} + k$) and $x(0) < a_0, y(0) < b_0, z(0) < c_0$.

Clearly, under this condition,

$$\inf\{|\vec{u}_i - \vec{u}_{i+1}| : \quad \vec{u}_i \in \partial\Pi_i, \ \vec{u}_{i+1} \in \partial\Pi_{i+1}\} \ge k > 0.$$

Let us explain why Condition 7.1 can be satisfied for an arbitrarily fixed $k > 0$.

Along with the parabolas as in Fig. 9, panel A, we introduce the expanded graphs (shown in Fig. 10, panel A with the dashed blue lines) of the functions

$$z = \frac{-1}{\beta_{13}e^k}\left[(1 - x)(x - \alpha_1) - \beta_{12}y_0 - \beta_{13}z_0\right];$$

$$x = \frac{-1}{\beta_{31}e^k}\left[(z_0 - z)(z - \alpha_2) - \beta_{32}y_0\right].$$

The right-hand parts become bigger than z and x for big enough x and z correspondingly, and one can choose $a_0 = c_0$ such that

$$a_0 = c_0 \quad < \quad \frac{-1}{\beta_{13}e^k}\left[(1-x)(x-\alpha_1) - \beta_{12}y_0 - \beta_{13}z_0\right];$$

$$a_0 = c_0 \quad < \quad \frac{-1}{\beta_{31}e^k}\left[(z_0 - z)(z-\alpha_2) - \beta_{32}y_0\right]$$

$$\text{and} \qquad a_0 > x(0), \qquad c_0 > z(0).$$

After that, the whole red square in Fig. 10, panel A, with $a_1 = a_0e^k$ and $c_1 = c_0e^k = a_1$, is within the area where the square brackets in the first and third equations (7) are negative. The image of Fig. 10, panel A on the plain (v_1, v_3) is given in Fig. 10, panel B. It remains to take

$$b_0 > \max\{y_0 + \beta_{21}a_1 + \beta_{23}(c_1 - z_0), \quad y(0)\}.$$

In general, for all $i \geq 1$, we put

$$a_i = a_{i-1}e^k, \qquad c_i = c_{i-1}e^k$$

$$\text{and} \qquad b_i = \max\{y_0 + \beta_{21}a_{i+1} + \beta_{23}(c_{i+1} - z_0), \quad b_{i-1}e^k\}.$$

The obtained sequence $\{(a_i, b_i, c_i)\}_{i=0}^\infty$ satisfies Condition 7.1.

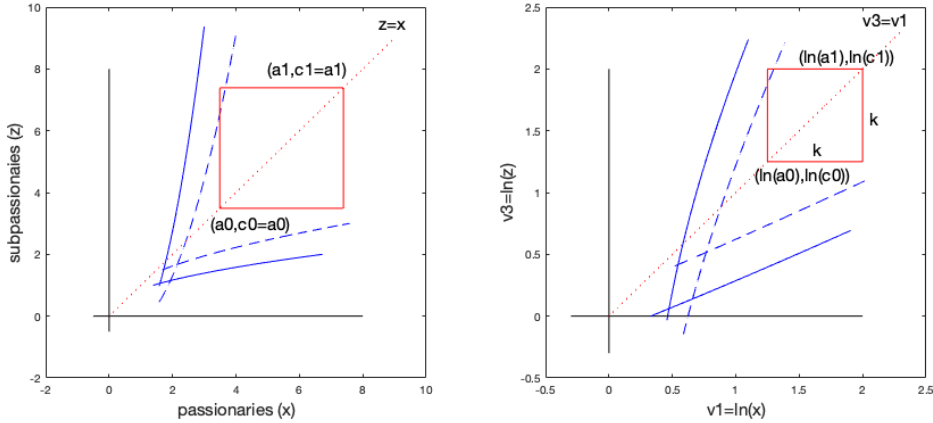Figure 10: Construction of the first prisms Π_0 and Π_1. Parameter values are as in Fig. 9; $k = 0.75$.

The SDE (14), for the prism Π_i, in its vector form means that

$$\vec{V}^i(t,\omega) = \vec{v}(0) + \int_0^t \vec{f^i}(\vec{V}^i(s,\omega))ds + \Xi\vec{W}(t,\omega) \qquad a.s. \tag{15}$$

for all $t \geq 0$. Here the functions $\vec{f^i} = (f_1^i, f_2^i, f_3^i)$ are constructed, as described above, for the prism Π_i. The vector notations are conventional, $\Xi = \begin{bmatrix} \sigma_1 & 0 & 0 \\ 0 & \sigma_2 & 0 \\ 0 & 0 & \sigma_3 \end{bmatrix}$. Similarly, we write down equations (10) as

$$\vec{V}(t,\omega) = \vec{v}(0) + \int_0^t \vec{f}(\vec{V}(s,\omega))ds + \Xi\vec{W}(t,\omega) \qquad a.s. \tag{16}$$

for all $t \geq 0$. Note that, if a random process $\vec{Z}(t,\omega)$ satisfies equation (15), then $\vec{V}^i(t,\omega) = \vec{Z}(t,\omega)$ for all $t \geq 0$ almost surely. (The processes $\vec{V}^i$ and $\vec{Z}$ are 'indistinguishable', often called 'versions' or 'modifications' [14].)

Suppose $\tau > 0$ is arbitrarily fixed, construct the process $\vec{V}$ on $[0,\tau]$, which satisfies equation (16), and prove that it is unique. The idea is as follows.

- *The process $\vec{V}$ will be a combination of the processes $\vec{V}^i$.*

- *Between the prisms Π_{i-1} and Π_i, the process $\vec{V}^i$ is pushed back to the prism Π_{i-1}, and the chance for it to reach the boundary of the prism Π_i is smaller than a constant $\varepsilon < 1$.*

- *Hence, almost surely, there is $j \geq 0$ such that the process $\vec{V}^j$ lives in the prism Π_j, where it is unique and coincides with $\vec{V}$.*

After that, one can extend the unique solution of equation (16) to infinite horizon $[0, \infty)$. Below, we omit some technical details. The more detailed proof can be found in [15].

We introduce 'debutes'

$$D_i(\omega) := \inf\{0 < t \leq \tau : \quad \vec{V}^i(t, \omega) \in \Pi_{i+1} \setminus \Pi_i\}, \quad i = 0, 1, \dots$$

and the (measurable) sets

$$\Omega_i := \{\omega \in \Omega : \quad D_i(\omega) \geq \tau\}, \quad i = 0, 1, \dots.$$

On each set Ω_i, for all $s \leq \tau$, $\vec{V}^i(s, \omega) \in \Pi_i$ meaning that $\vec{f}^i(\vec{V}^i(s, \omega)) = \vec{f}(\vec{V}^i(s, \omega))$ and, by (15), for all $t \leq \tau$, for P-almost all $\omega \in \Omega_i$,

$$\vec{V}^i(t, \omega) = \vec{v}(0) + \int_0^t \vec{f}(\vec{V}^i(s, \omega))ds + \Xi \vec{W}(t, \omega). \tag{17}$$

For $0 \leq s \leq \tau$, we put

$$\begin{aligned}
\vec{V}(s, \omega) &:= \vec{V}^0(s, \omega) \text{ on } \Omega_0 \quad \text{and} \\
\vec{V}(s, \omega) &:= \vec{V}^i(s, \omega) \text{ on } \overline{\cup_{j=0}^{i-1}\Omega_j} \cap \Omega_i \quad \text{for } i = 1, 2, \dots.
\end{aligned}$$

As the result, the continuous process $\vec{V}$ is built on $\cup_{i=0}^\infty \Omega_i$.

First, we are going to show show that

$$P\left(\bigcup_{i=0}^\infty \Omega_i\right) = 1. \tag{18}$$

For $i \geq 1$, let us introduce debutes

$$D_{i,i-1}(\omega) := \inf\{0 < t \leq \tau : \vec{V}^i(t, \omega) \in \Pi_i \setminus \Pi_{i-1}\}$$

and the corresponding subsets

$$\Omega_{i,i-1} := \{\omega \in \Omega : \quad D_{i,i-1}(\omega) \geq \tau\}.$$

For each $i \geq 1$, within the prism Π_{i-1}, the SDE (15) for the processes $\vec{V}^i$ and $\vec{V}^{i-1}$ is the same. Therefore, one can show that $\vec{V}^i = \vec{V}^{i-1}$ for all $t \in [0, \tau]$ almost surely on $\Omega_{i,i-1} \cup \Omega_{i-1}$, and

$$P(\Omega_{i-1} \triangle \Omega_{i,i-1}) = 0. \tag{19}$$

Moreover, for each $i = 0, 1, 2, \dots$, $\vec{V} = \vec{V}^i$ for all $t \in [0, \tau]$ almost surely on Ω_i.

Let $i \geq 1$ be arbitrarily fixed and explain why

$$P(\overline{\Omega_i}) \leq \varepsilon P(\overline{\Omega_{i-1}}), \tag{20}$$

for an i-independent constant $\varepsilon < 1$, provided k as in Condition 7.1 is big enough:

$$\frac{4}{\sqrt{2\pi}} \int_{d_j}^\infty e^{-\frac{y^2}{2}} dy < \frac{1}{3}, \quad j = 1, 2, 3, \tag{21}$$

where $d_j = \frac{k}{2\sigma_j \sqrt{\tau}}$.

Suppose that $\omega \in \overline{\Omega_i}$ and $V_1^i(D_i(\omega), \omega) = \ln a_i$, i.e.

$$\omega \in E_1 := \{\omega : \ V_1^i(D_i(\omega), \omega) = \ln a_i\}.$$

Other cases when $\ln a_i$ is replaced with $\ln b_i$ or $\ln c_i$, leading to the sets E_2 and E_3, can be studied similarly. Clearly $\overline{\Omega_i} \subset \overline{\Omega_{i,i-1}}$ and, for $\omega \in \overline{\Omega_i}$, $0 < D_{i,i-1}(\omega) < D_i(\omega) < \tau$. Let $\vec{U}(\omega) := \vec{V}^i(D_{i,i-1}(\omega), \omega) \in \partial\Pi_{i-1}$. Since $\omega \in E_1$, we introduce

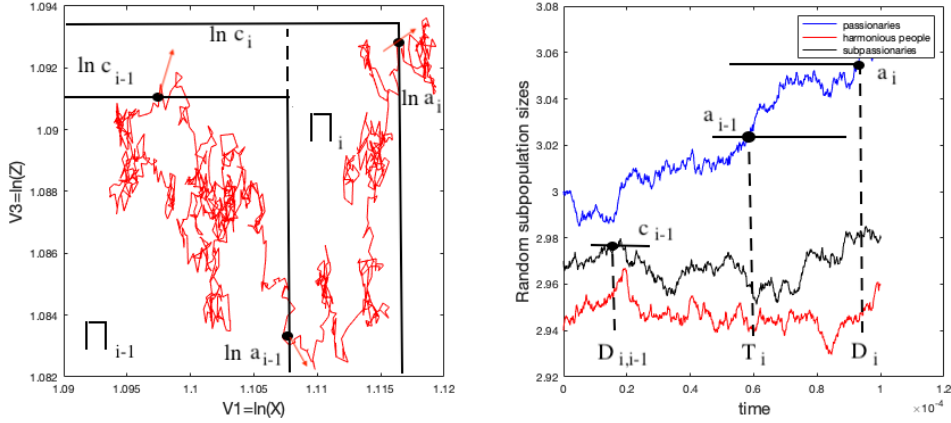$$T_i(\omega) := \sup\{t \in [D_{i,i-1}(\omega), D_i(\omega)] : \ V_1^i(t, \omega) \leq \ln a_{i-1}\}.$$

Figure 11: Small fragment of the motion of $\vec{V}^i$: phase trajectories on panel A and time trajectories on Panel B. The black spots correspond to the time moments $D_{i,i-1}$, T_i and D_i; $\vec{U} = \ln c_{i-1}$. The red arrows at the spots on panel A show the direction of the movement of the phase trajectories at the time moments $D_{i,i-1}$, T_i and D_i. Parameter values: $\alpha_1 = 0.03$, $\alpha_2 = 0.11$, $y_0 = 0.075$, $z_0 = 0.22$, $\beta_{12} = -6$, $\beta_{13} = 0.6$, $\beta_{21} = 0.2$, $\beta_{23} = 0.1$, $\beta_{31} = 0.5$, $\beta_{32} = 0$, $\gamma_1 = 1$, $\gamma_2 = 0.7$, $\gamma_3 = 0.2$, $\sigma_1 = \sigma_2 = \sigma_3 = 1$.

These objects are illustrated in Fig. 11: the process $\vec{V}^i$ leaves the prism Π_{i-1} for the first time when $V_3^i(D_{i,i-1}) = \ln c_{i-1}$, it leaves the prism Π_i when $V_1^i(D_i) = \ln a_i$, and between the time moments T_i and D_i, the first component satisfies inequalities $\ln a_{i-1} \leq V_1^i \leq \ln a_i$ and $V_1^i(T_i) = \ln a_{i-1}$. Now

$$
\begin{aligned}
\ln a_i &= V_1^i(D_i) = V_1^i(T_i) + \int_{T_i}^{D_i} f_1^i(\vec{V}^i(s))ds + \sigma_1[W_1(D_i)) - W_1(T_i)] \\
&\leq \ln a_{i-1} + \sigma_1[W_1(D_i) - W_1(T_i)]
\end{aligned}
$$

because $f_1^i \leq 0$ within the prism Π_i (see Condition 7.1). Therefore, on the time interval $[T_i, D_i] \subset [0, \tau]$ the Brownian motion has the variation bigger than $\frac{k}{\sigma_1}$ because $\ln a_i \geq \ln a_{i-1} + k$. According to (21), we deduce that, for each $\vec{u} \in \partial\Pi_{i-1}$ (the value of $\vec{U}(\omega)$),

$$
\begin{aligned}
P(E_1|\vec{u}) &= \delta < \frac{1}{3}; \\
P(\overline{\Omega_i}|\vec{u}) &\leq P(E_1 \cup E_2 \cup E_3|\vec{u}) \leq \varepsilon := 3\delta < 1
\end{aligned}
$$

and

$$P(\overline{\Omega_i}) = \int_{\overline{\Omega_{i,i-1}}} P(\overline{\Omega_i}|\vec{U}(\omega)) \, dP(\omega) \leq \varepsilon P(\overline{\Omega_{i,i-1}}).$$

Inequality (20) now follows from (19).

Using (20), we have

$$P\left(\bigcap_{i=0}^{\infty}\overline{\Omega_i}\right) = \lim_{N\to\infty} P\left(\bigcap_{i=0}^{N}\overline{\Omega_i}\right) \leq \lim_{N\to\infty} P(\overline{\Omega_N}) \leq \lim_{N\to\infty}\varepsilon^N P(\overline{\Omega_0}) = 0.$$

Therefore, $P\left(\bigcup_{i=0}^{\infty}\Omega_i\right) = 1 - P\left(\bigcap_{i=0}^{\infty}\overline{\Omega_i}\right) = 1$, and equality (18) is proved. The more rigorous and detailed reasoning can be found in [15].

According to (17), the constructed continuous process $\vec{V}(t,\omega)$ satisfies equation (16) (and (10)) for all $t \in [0,\tau]$ a.s., i.e., it is a strong continuous solution to those SDEs. If $\vec{Z}$ is another strong continuous solution, then it is bounded on $[0,\tau]$ and hence belongs to some prism Π_i. As the result, $\vec{Z} = \vec{V}_i = \vec{V}$ for all $t \in [0,\tau]$ a.s. on Ω_i, i.e. $\vec{Z} = \vec{V}$ for all $t \in [0,\tau]$ a.s. on $\bigcup_{i=0}^{\infty}\Omega_i$ and on Ω (see (18)). For more accurate reasoning see [15].

Finally, extension to the infinite horizon $[0,\infty)$ of the solution $\vec{V}$ to the SDE (16) (and (10)) is trivial. Take an increasing sequence $\{\tau_j\}_{j=1}^{\infty}$, $\tau_j > 0$, with $\lim_{j\to\infty}\tau_j = \infty$, construct the solutions $\vec{V}^{\tau_j}$ to SDE (16) (and (10)) on the intervals $[0,\tau_j]$ and put

$$\vec{V}(t,\omega) := \vec{V}^{\tau_j}(t,\omega)\mathbb{I}\{t \in [\tau_{j-1},\tau_j)\},$$

where $\tau_0 := 0$. If there is another process $\vec{Z}$ satisfying this property then, due to the uniqueness of $\vec{V}^{\tau_j}$, $\vec{Z}(t,\omega) = \vec{V}^{\tau_j}(t,\omega)$ for all $t \in [\tau_{j-1},\tau_j)$ a.s., $j = 1, 2, \ldots$. Hence $\vec{Z}(t,\omega) = \vec{V}(t,\omega)$ for all $t \in [0,\infty)$ a.s.

The proof is completed.

References

[1] M.Artzrouni and J.Komlos. The formation of the European state system, a spatial "predatory" model. *Historical Methods*, **29**(3), pp. 126-134, 1996.

[2] S.Bowles. Group competition, reproductive leveling, and the evolution of human altruism. *Science*, **314**, pp. 1569-1572, 2006.

[3] R.Collins. Prediction in macrosociology - the case of the Soviet collapse. *Americal Journal of Sociology*, **100**(6), pp. 1552-1593, 1995.

[4] R.J.Elliott. *Stochastic Calculus and Applications*. Springer-Verlag, NY etc, 1982.

[5] L.Feuchtwanger. *Raquel, the Jewess of Toledo*. New York Messner, 1956.

[6] R.Fitzhugh. Impulses and physiological states in theoretical models of nerve membrane. *Biophysical Journal*, **1**(6), pp. 445-466, 1961.

[7] E.Gellner. *Muslim Society*. Cambridge University Press, Cambridge, 1981.

[8] L.Gumilev. *Ethnogenesis and the Biosphere*. Progress Publishers, Moscow, 1990.

[9] L.N.Gumilev and K.P.Ivanov. Ethnic-processes – the approaches in researches. *Sotsiologicheskie Issledovaniya*, 1, pp.50–57, 1992, (in Russian).

[10] A.K.Guz and L.A.Pautova. *Global Ethnosociology*. Librokom, Moscow, 2019, (in Russian).

[11] Ibn Khaldun. *The Muqaddimah: An Introduction to History*. Pantheon Books, New York, 1958.

[12] V.Lefebvre. Theoretical modeling of the subject: Western and Eastern types of human reflexion. *Progress in Biophysics and Molecular Biology*, **131**, pp. 325-335, 2017.

[13] J.D.Murray. *Mathematical Biology I. An Introduction*. Springer, New York, 2002.

[14] B.Oksendal. *Stochastic Differential Equations*. Springer, Heidelberg, 2013.

[15] A.Piunovskiy and B.Vasiev. *Modelling Ethnogenesis.* arXiv:2201.12873

[16] R.Putnam. *Bowling Along. The Collapse and Revival of American Community.* Simon and Schuster, New York, 2000.

[17] O.Spengler. *The Decline of the West.* Arktos Media Ltd, 2021.

[18] R.Taagepera. Extraction and contraction patterns of large polities. *International Studies Quarterly*, **41**, pp. 475-504, 1997.

[19] G.Teschl. *Ordinary Differential Equations and Dynamical Systems.* AMS, Rhode Island, 2012.

[20] L.Tolstoy. *War and Peace.* Penguin Classics, 2016.

[21] A.Toynbee. *A Study of History.* Oxford University Press, 1987.

[22] H.Triandis. *Individualism and Collectivism.* Westview, Boulder, 1995.

[23] P.Turchin. *Historical Dynamics.* Princeton University Press, New Jercey, 2003.

[24] P.Turchin. A theory for formation of large empires. *Journal of Global History.* **4**, pp. 191–217, 2009.

[25] P.J.Wangersky. Lotka-Volterra population models. *Annual Review of Ecology and Systematics*, **9**, pp.189-218, 1978.

[26] Q.Zhang and D.Jiang. Analysis of autonomous Lotka-Volterra systems by Levy noise. *J. of Applied Analysis and Computation*, **11**, pp.176-191, 2021.